

# Very Small Wide-Band MMIC Magic T's Using Microstrip Lines on a Thin Dielectric Film

TAKAHIRO HIRAKA, MEMBER, IEEE, TSUNEO TOKUMITSU, MEMBER, IEEE,  
AND MASAYOSHI AIKAWA, MEMBER, IEEE

**Abstract**—A newly developed MMIC magic T (180° hybrid circuit) using microstrip lines on a thin silicon oxynitride (SiON) dielectric film has been proposed. The microstrip line area reduction is achieved by using very narrow line width thin-film microstrip (TFMS) lines, derived from the thin substrate structure. The area is effectively minimized using meander-like configurations. The SiON thin film is successfully deposited by low-temperature plasma CVD. The MMIC magic T has been designed for a center frequency of 12 GHz, and small size with wide-band performance from 6 GHz to 18 GHz has been achieved. Thus, magic T's using thin-film microstrip lines are promising for miniaturized high-performance MMIC's, such as balanced mixers and modulators.

## I. INTRODUCTION

THE MAGIC T (180° hybrid circuit) is a fundamental and important circuit in microwave and millimeter-wave equipment. Conventional magic T's realized by "double-sided microwave integrated circuit (MIC)" technology have been reported [1], [2]. These magic T's use a combination of various transmission lines on both sides of the substrate. MMIC magic T's which employ a combination of coplanar waveguides and slotlines on one side of a substrate [3] have also been reported. However, the latter need a large chip size, because the quarter-wavelength microstrip and coplanar lines are formed on rather thick (several hundred micrometers) substrates. In order to reduce the chip area of such transmission lines, a line unified FET (LUFET) MMIC magic T which employs a unique FET electrode configuration and an active matching technique was recently proposed by two of the authors [4], [5]. In the frequency range from 20 GHz into the millimeter-wave band, the active matching technique is not suitable, because present active devices have operating frequency limitations.

In this paper, a very small wide-band MMIC magic T is proposed. The magic T employs thin-film microstrip

(TFMS) lines, which are formed on a thin dielectric film deposited on a GaAs substrate. A silicon oxynitride (SiON) is used for the thin dielectric film due to its low film stress, easy deposition, and low-temperature processing. The features of the magic T are as follows. It 1) significantly reduces chip size due to very narrow TFMS line width, 2) exhibits wide-band dividing/coupling characteristics, and 3) promises millimeter-wave band applications.

This paper describes the MMIC magic T configuration, the characteristics of the TFMS, MMIC magic T design and fabrication, and the results at the center frequency of 12 GHz.

## II. MAGIC T CONFIGURATION

The proposed MMIC magic T using TFMS lines is shown in Fig. 1. This magic T is composed of a slotline series T junction, a microstrip parallel T junction, and two quarter-wavelength TFMS lines, which combine the series and parallel T junctions. The TFMS lines are fabricated using a thin SiON dielectric film deposited on the slotline T junction. Ports (E) and (H) correspond to the E and H arms of a metallic waveguide magic T, respectively, and ports (1) and (2) are the remaining two ports. Fig. 2(a) and (b) shows equivalent circuits to explain the circuit behavior. In this figure, arrows schematically express input and output signal polarities. The out-of-phase mode (Fig. 2(a)) is excited by a signal into port (E) or, conversely, by out-of-phase signals of the same amplitude into ports (1) and (2). The in-phase mode (Fig. 2(b)) is excited by a signal into port (H) or, conversely, by in-phase signals of the same amplitude into ports (1) and (2). As shown in Fig. 2, ports (E) and (H) are electrically isolated due to the orthogonal mode effect. Essentially the quarter-wavelength transmission lines are required because electrically shorted port (H) must be isolated from the other ports in the out-of-phase mode. The proposed magic T achieves a drastic size reduction of the quarter-wavelength transmission lines by using the very narrow width TFMS lines and

Manuscript received December 29, 1988; revised March 29, 1989.

T. Hiraoka and T. Tokumitsu are with the ATR Optical and Radio Communications Research Laboratories, Inuidani, Seika-cho, Soraku-gun, Kyoto 61902, Japan.

M. Aikawa is with the NTT Radio Communication Systems Laboratories, Take 1-2356, Yokosuka, Kanagawa 238-03 Japan.

IEEE Log Number 8929890.

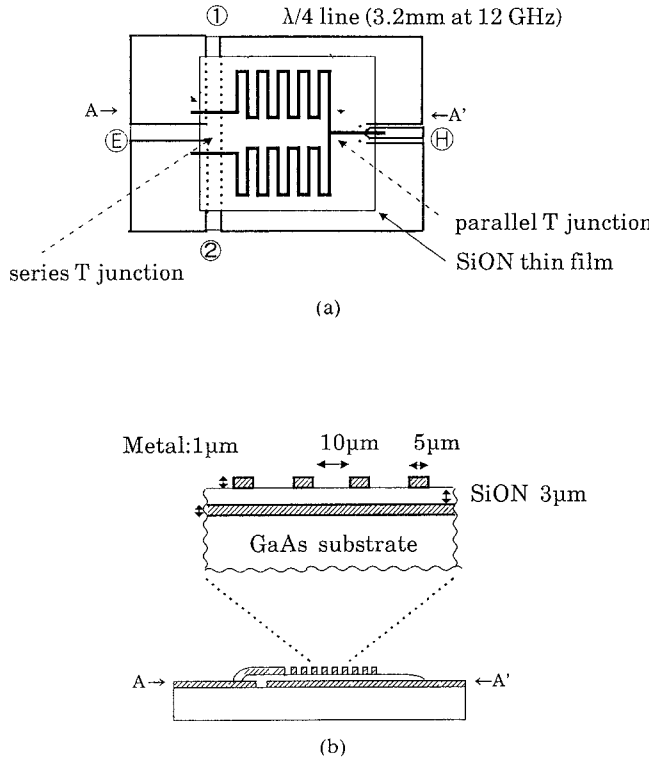


Fig. 1. Proposed MMIC magic T using microstrip lines on a thin dielectric film. (a) Top view. (b) Cross-sectional view.

the meanderlike configuration of the TFMS lines, made possible by the thin substrate structure.

The basic design of this magic T, where TFMS lines are assumed to be lossless transmission lines, is achieved through orthogonal mode analysis based on a symmetrical configuration with respect to ports  $(\mathbb{E})$  and  $(\mathbb{H})$ . Fig. 3(a) and (b) shows the equivalent circuits in the out-of-phase and in-phase mode excitations, respectively. The reflection coefficients at port  $(\mathbb{1})$  derived from each mode are used in the magic T design. When  $\Gamma_{++}$  and  $\Gamma_{+-}$  are the in-phase mode and out-of-phase mode reflection coefficients at port  $(\mathbb{1})$  in Fig. 3, respectively, the return loss at ports  $(\mathbb{1})$  and  $(\mathbb{2})$  and the isolation between ports  $(\mathbb{1})$  and  $(\mathbb{2})$  are given as follows:

$$\text{return loss (ports } (\mathbb{1}), (\mathbb{2}) \text{)} = 20 \log_{10} \frac{1}{2} |\Gamma_{++} + \Gamma_{+-}| \text{ (dB)} \quad (1)$$

$$\text{isolation (ports } (\mathbb{1}) - (\mathbb{2}) \text{)} = 20 \log_{10} \frac{1}{2} |\Gamma_{++} - \Gamma_{+-}| \text{ (dB).} \quad (2)$$

Because the circuit is reciprocal, impedance matching at each port and isolation between ports  $(\mathbb{1})$  and  $(\mathbb{2})$  are also accomplished when the absolute factor of both equations equals zero at the center frequency.  $\Gamma_{++}$  and  $\Gamma_{+-}$  are

given as follows:

$$\Gamma_{++} = \frac{(2Z_{0(\mathbb{H})} - Z_{0(\mathbb{1})})^2 + j(Z_{0\text{TFMS}}^2 - 2Z_{0(\mathbb{1})}Z_{0(\mathbb{H})}) \tan \theta_{\text{TFMS}}}{(2Z_{0(\mathbb{H})} + Z_{0(\mathbb{1})})^2 + j(Z_{0\text{TFMS}}^2 + 2Z_{0(\mathbb{1})}Z_{0(\mathbb{H})}) \tan \theta_{\text{TFMS}}} \quad (3)$$

$$\Gamma_{+-} = \frac{-Z_{0(\mathbb{E})}Z_{0(\mathbb{1})} - jZ_{0\text{TFMS}}(Z_{0(\mathbb{E})} - 2Z_{0(\mathbb{1})}) \cot \theta_{\text{TFMS}}}{Z_{0(\mathbb{E})}Z_{0(\mathbb{1})} - jZ_{0\text{TFMS}}(Z_{0(\mathbb{E})} + 2Z_{0(\mathbb{1})}) \cot \theta_{\text{TFMS}}}. \quad (4)$$

As a result, the following conditions are derived through the above design procedure:

$$Z_{0(\mathbb{E})} = 2Z_{0(\mathbb{1})} \quad (5)$$

$$Z_{0\text{TFMS}} = \sqrt{(2Z_{0(\mathbb{H})})Z_{0(\mathbb{1})}} \quad \theta_{\text{TFMS}} = \pi/2. \quad (6)$$

When  $Z_{0(\mathbb{1})} = Z_{0(\mathbb{2})} = Z_{0(\mathbb{H})} = 50 \Omega$ ,  $Z_{0(\mathbb{E})}$  is  $100 \Omega$ ,  $Z_{0\text{TFMS}}$  is  $70 \Omega$ , and  $\theta_{\text{TFMS}}$  is a quarter wavelength at the center frequency. Fig. 4 shows magic T performance calculated according to the above conditions. The relative operating frequency range reaches 100 percent in the frequency region where the return loss and the isolation between ports  $(\mathbb{1})$  and  $(\mathbb{2})$  are greater than 10 dB.

### III. CHARACTERISTICS OF TFMS

The characteristics of the TFMS for a practical design of the proposed MMIC magic T are discussed in this section. TFMS lines are not lossless; rather they are lossy transmission lines. The loss is as much as ten times higher than that of microstrip lines fabricated on the  $100\text{-}\mu\text{m}$ -thick GaAs substrate shown below. The loss characteristics are effectively used to realize the wide-band impedance matching and isolation characteristics.

The measured insertion loss of the TFMS line as a function of frequency is shown in Fig. 5, where the line length  $L$ , the line width  $w$ , and the metal thickness  $t$  of the TFMS line are  $1.5 \text{ mm}$ ,  $5 \mu\text{m}$ , and  $1 \mu\text{m}$ , respectively, and the SiON dielectric film thickness  $H$  is  $3 \mu\text{m}$ . The TFMS characteristic impedance is  $50 \Omega$ . The solid line represents the measured loss, and the dotted line the loss calculated using conventional approximate formulas [6]–[8], where a surface resistivity  $R_s$  proportional to the square root of the frequency  $f$  is used ( $R_s = \sqrt{\pi\mu_0\rho f}$ ). The measured insertion loss is about  $1 \text{ dB}$  at frequencies from dc to  $20 \text{ GHz}$ . The value increases gradually from  $0.8 \text{ dB}$  at dc to  $1.2 \text{ dB}$  at  $20 \text{ GHz}$ . In the frequency range from  $10$  to  $20 \text{ GHz}$ , the measured loss increases along with the calculated loss. However, the loss has a nearly constant value from dc to  $10 \text{ GHz}$ . The difference between the measured and calculated losses indicates that the approximate formula does not characterize TFMS with a metal thickness of  $1 \mu\text{m}$ , which is thinner than the skin depth in the frequency range.

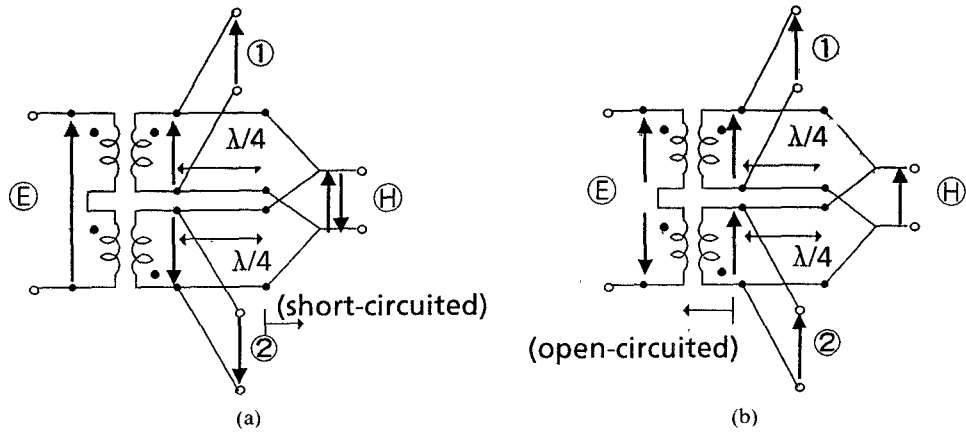


Fig. 2. Equivalent magic T circuits. (a) 180° out-of-phase mode. (b) In-phase mode.

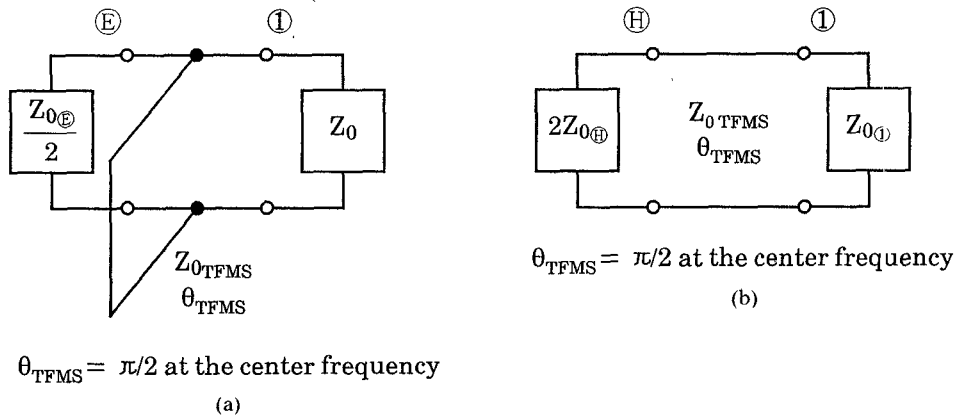


Fig. 3. Equivalent magic T circuits. (a) Out-of-phase mode excitation. (b) In-phase mode excitation.

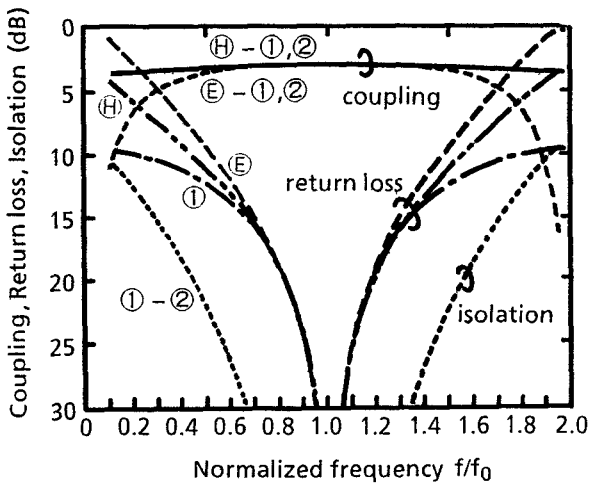


Fig. 4. Calculated performance of the magic T.

The total current  $I$  which flows through the cross section of the line is given by

$$I = I_0 \int_0^t e^{-x/\delta} dx = I_0 \delta (1 - e^{-t/\delta}) \quad (7)$$

where  $I_0$  is the current density on the surface of the metal,  $t$  is the thickness of the metal, and  $\delta$  is the skin depth, represented as  $\delta = 1/\sqrt{\pi\mu_0\sigma f}$ , where  $\mu_0$  and  $\sigma$  are the magnetic permeability of free space and the conductivity

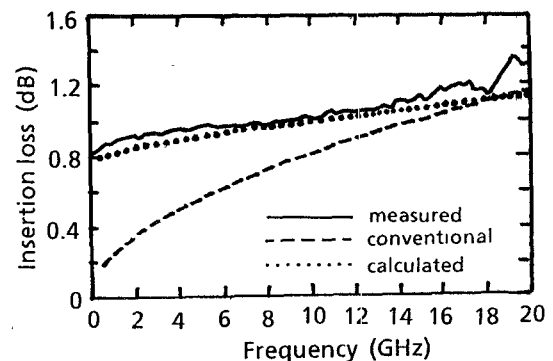


Fig. 5. TFMS experiment and calculated results.

of the metal, respectively. We define the skin depth of the TFMS,  $\delta'$ , as shown in the following equation, because  $I = I_0 \delta$  when  $t$  is sufficiently large compared to  $\delta$ :

$$\delta' = \delta \times \left(1 - \exp \left[ - \frac{t}{\delta} \right]\right). \quad (8)$$

From this definition, surface resistivity  $R_s(f)$  of the TFMS line is obtained as follows:

$$R_s(f) = \frac{\rho}{\delta'} = \frac{\sqrt{\pi\mu_0\sigma f}}{1 - e^{-t/\delta}} \quad (\Omega/\square) \quad (9)$$

where  $\rho$  is the resistivity of the metal, which is recipro-

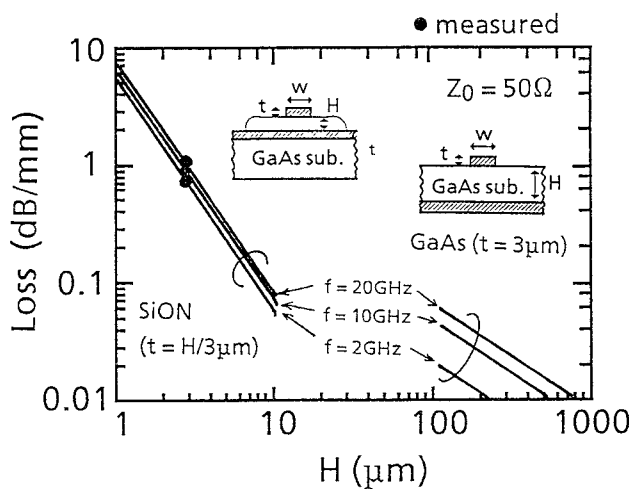


Fig. 6. Characteristics of TFMS and conventional microstrip lines.

cally equal to  $\sigma$ . By using the surface resistivity for dc current,  $R_{s0}$ , (9) can be written as

$$R_s(f) = R_{s0} \times \frac{tK\sqrt{f}}{1 - e^{-tK\sqrt{f}}} \quad (\Omega/\square) \quad (10)$$

where  $K = \sqrt{\pi\mu_0\sigma}$ . The losses calculated using (10), which are shown in Fig. 5, closely agree with the measured losses, where  $R_{s0} = 0.029 \Omega/\square$ ,  $t = 1 \mu\text{m}$ , and  $\rho = 2.4 \times 10^{-6} \Omega \cdot \text{cm}$ .

The loss characteristics of the TFMS line as a function of the film thickness, compared with a conventional microstrip line on a GaAs substrate, are shown in Fig. 6. The metal thickness  $t$  of the TFMS line is assumed to equal  $H/3$ . This assumption is reasonable when other thin films are stacked onto the TFMS for multilayer MMIC's. The metal thickness of the microstrip line fabricated on a GaAs substrate is maintained at a constant value, that is,  $3 \mu\text{m}$ . All characteristics are calculated for  $50 \Omega$  lines. The dots in Fig. 6 show the measured loss for the TFMS line on a  $3\text{-}\mu\text{m}$ -thick SiON film. By increasing the film thickness to  $6 \mu\text{m}$ , the TFMS loss will be reduced 90 percent, which is approximately equal to that of a microstrip line on a  $100\text{-}\mu\text{m}$ -thick GaAs substrate.

We discuss the area of TFMS lines on a SiON film and conventional microstrip lines on a GaAs substrate. Fig. 7 shows the estimated area of the TFMS lines and microstrip lines as a function of film thickness  $H$ . In this estimation, the "area" is defined as the product of three line widths times a quarter-wavelength, where each transmission width is determined by the point at which the line impedance is  $50 \Omega$ . The SiON film dielectric constant is 5.0, and that of GaAs is 12.9. The area of TFMS lines on a  $6\text{-}\mu\text{m}$ -thick SiON, for example, is about  $1/10$  that of conventional microstrip lines on a  $100\text{-}\mu\text{m}$ -thick GaAs substrate.

#### IV. MAGIC T DESIGN

Performance of the magic T using TFMS has been calculated to estimate the effects of the loss due to the TFMS configuration. The port impedances derived in Sec-

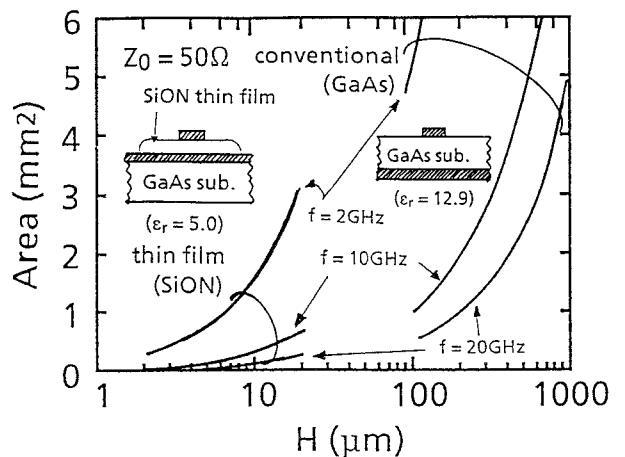
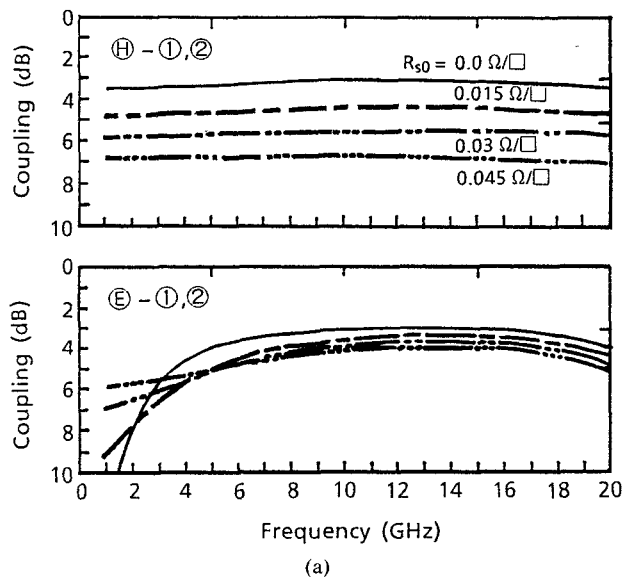


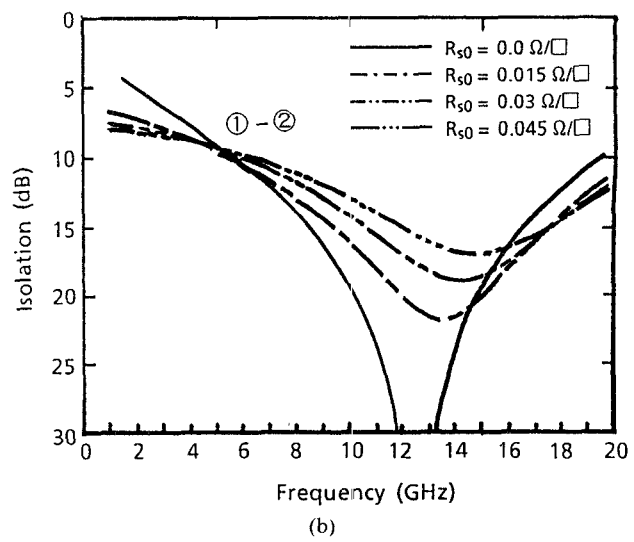
Fig. 7. Chip area of TFMS and conventional microstrip lines.

tion II are used in the calculations ( $Z_{0(2)} = 100 \Omega$ ,  $Z_{0(1)} = Z_{0(2)} = Z_{0(H)} = 50 \Omega$ ,  $Z_{0\text{TFMS}} = 70 \Omega$ ). The line width of the  $70 \Omega$  TFMS line is  $2.1 \mu\text{m}$  and the value of  $R_{s0}$  is  $0.03 \Omega/\square$  when the SiON film and the metal thickness are  $3 \mu\text{m}$  and  $1 \mu\text{m}$ , respectively. The results are shown in Fig. 8, where  $R_{s0}$  varies from  $0 \Omega/\square$  to  $0.45 \Omega/\square$  in the calculations. Fig. 8(a) shows the frequency characteristics of the coupling from port  $(E)$  or  $(H)$  to ports  $(1)$  and  $(2)$ . The in-phase coupling from port  $(H)$  to ports  $(1)$  and  $(2)$  drops sharply according to the increase in  $R_{s0}$ , retaining flat frequency characteristics for  $R_{s0} = 0 \Omega/\square$ , while the out-of-phase coupling from port  $(E)$  to ports  $(1)$  and  $(2)$  drops gradually, thus smoothing the curve. Fig. 8(b) shows the frequency characteristics of the isolation between ports  $(1)$  and  $(2)$ . The isolation between ports  $(1)$  and  $(2)$  rises gradually and smooths the curves. Fig. 8(c) shows the frequency characteristics of the return loss at ports  $(E)$  and  $(H)$ . The return loss characteristics at port  $(E)$  are poor at frequencies below 5 GHz when  $R_{s0} = 0 \Omega/\square$ . The increase in the value of  $R_{s0}$  improves this characteristic. The return loss at port  $(H)$  is greater than 10 dB for every  $R_{s0}$  in the frequency range from dc to 20 GHz. The increase in  $R_{s0}$  acts to increase the return loss at low frequencies while decreasing the return loss at higher frequencies. Fig. 8(d) shows the frequency characteristics of the return loss at ports  $(1)$  and  $(2)$ . Although the return loss changes sharply, it is still greater than 10 dB for every  $R_{s0}$  in the frequency range from 8 to 20 GHz.

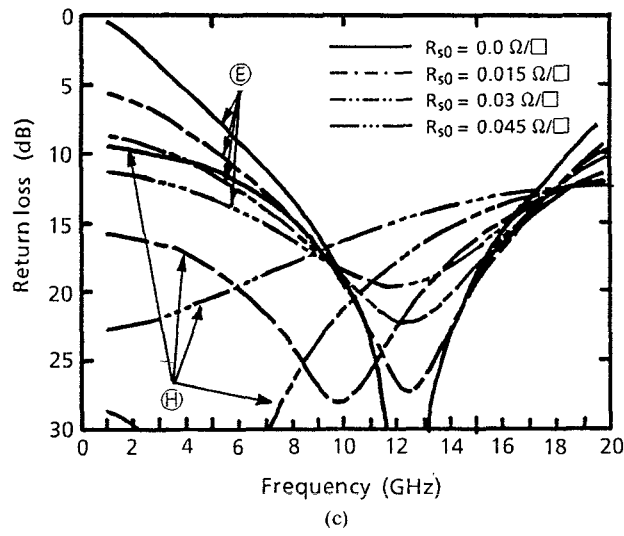
As estimated above, the performance of the magic T, with the exception of that of the couplings, is not particularly degraded by the loss of the TFMS. Therefore, the maximum value of  $R_{s0}$  is determined from the design requirements for the maximum coupling loss  $L_{\max}$  and the maximum difference  $\Delta L_{\max}$  between the couplings from port  $(E)$  or  $(H)$  to ports  $(1)$  and  $(2)$ . In our design an  $L_{\max}$  of 5 dB and a  $\Delta L_{\max}$  of 1 dB were chosen. These requirements are satisfied when  $R_{s0}$  is less than  $0.015 \Omega/\square$ . However, the  $70 \Omega$  TFMS line with a  $2.1 \mu\text{m}$  line width has a greater value of  $R_{s0}$  than required, that is,  $0.03 \Omega/\square$ .



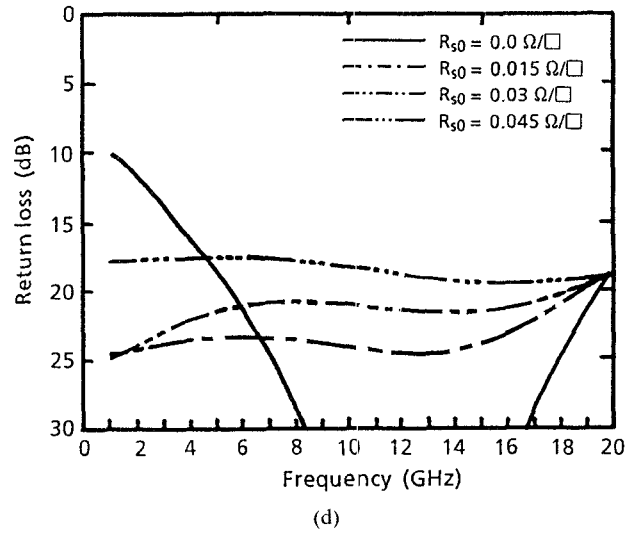
(a)



(b)

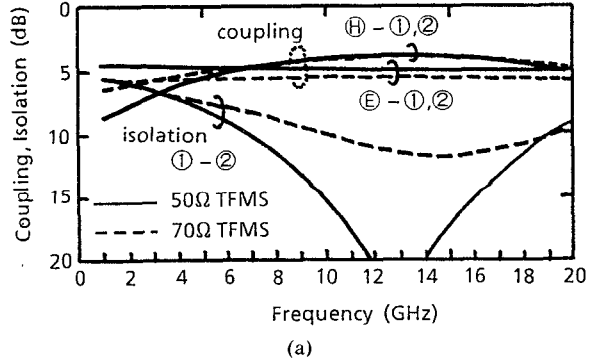


(c)

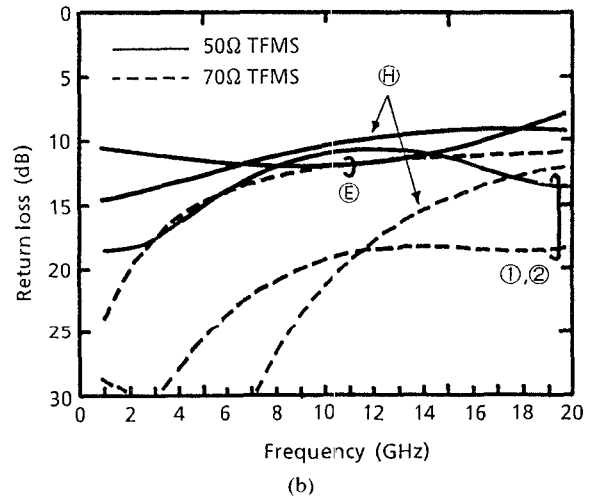


(d)

Fig. 8. Calculated performance of magic T. (a) Coupling between ports  $\textcircled{E}$ -①, ②, and  $\textcircled{H}$ -①, ②. (b) Isolation between ports ① and ②. (c) Return loss at ports  $\textcircled{E}$  and  $\textcircled{H}$ . (d) Return loss at ports ① and ②.



(a)



(b)

Fig. 9. Calculated performance of the magic T with 50  $\Omega$  and 70  $\Omega$  TFMS line. (a) Coupling and isolation. (b) Return loss.

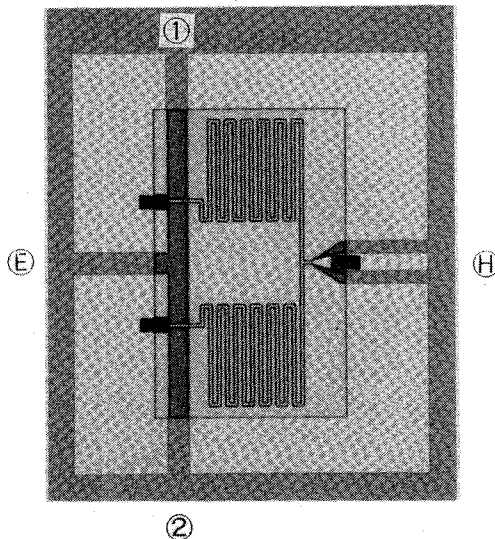


Fig. 10. Photomicrograph of a fabricated MMIC magic T (chip size:  $0.9 \text{ mm} \times 1.0 \text{ mm}$ ).

## V. FABRICATION AND RESULTS

The MMIC magic T shown in Fig. 1 was designed and fabricated by using TFMS lines with a 3- $\mu\text{m}$ -thick SiON film. As mentioned in Section IV, the 70  $\Omega$  TFMS loss is excessive. Therefore, a 50  $\Omega$  TFMS is chosen for magic T design, because the loss of 50  $\Omega$  TFMS with a 3- $\mu\text{m}$ -thick SiON film is improved over that of a 70  $\Omega$  TFMS. The slotline impedance of a port ④ is also 50  $\Omega$  in order to perform on-wafer measurement with an impedance of 50  $\Omega$ . Fig. 9 shows calculated performance of the magic T with port ④ impedance of 50  $\Omega$  instead of 100  $\Omega$ . Dotted lines indicate performance when the TFMS line impedance is 70  $\Omega$ , while solid lines indicate performance when the TFMS line impedance is 50  $\Omega$ . Although the choice of a 50  $\Omega$  TFMS instead of a 70  $\Omega$  TFMS may worsen the return loss of every port, a better than 10 dB (better than 9 dB for port ④) return loss is obtained. On the other hand, coupling and isolation between ports ① and ②, shown in Fig. 9(a), indicate that the choice of a 50  $\Omega$  TFMS line is effective for realizing the required  $L_{\max}$  and  $\Delta L_{\max}$  and better isolation characteristics.

Fabrication of TFMS is achieved by using a low-temperature plasma CVD deposited SiON film. The plasma CVD processed SiON film is chosen because (1) dielectric film damaged on a GaAs substrate, such as peeling and cracking, can be minimized, because SiON film stress (tensile  $1.7 \times 10^9 \text{ dyne/cm}^2$ ) is much lower than that of other insulators such as  $\text{SiO}_2$  or  $\text{Si}_3\text{N}_4$  on a GaAs substrate; (2) it is easy to control film thickness; and (3) the low-temperature (up to 350°C) process can be combined with a GaAs active device. A photomicrograph of a fabricated MMIC magic T is shown in Fig. 10. The design center frequency is 12 GHz. The total length of the quarter-wavelength TFMS line is 3.2 mm. The width and the line spacing in the meanderlike configuration are 5  $\mu\text{m}$  and 10  $\mu\text{m}$ , respectively. The thickness of evaporated metal is 1  $\mu\text{m}$ . The chip size is  $0.9 \times 1.0 \text{ mm}^2$  (the intrinsic area is only  $0.3 \times 0.5 \text{ mm}^2$ ).

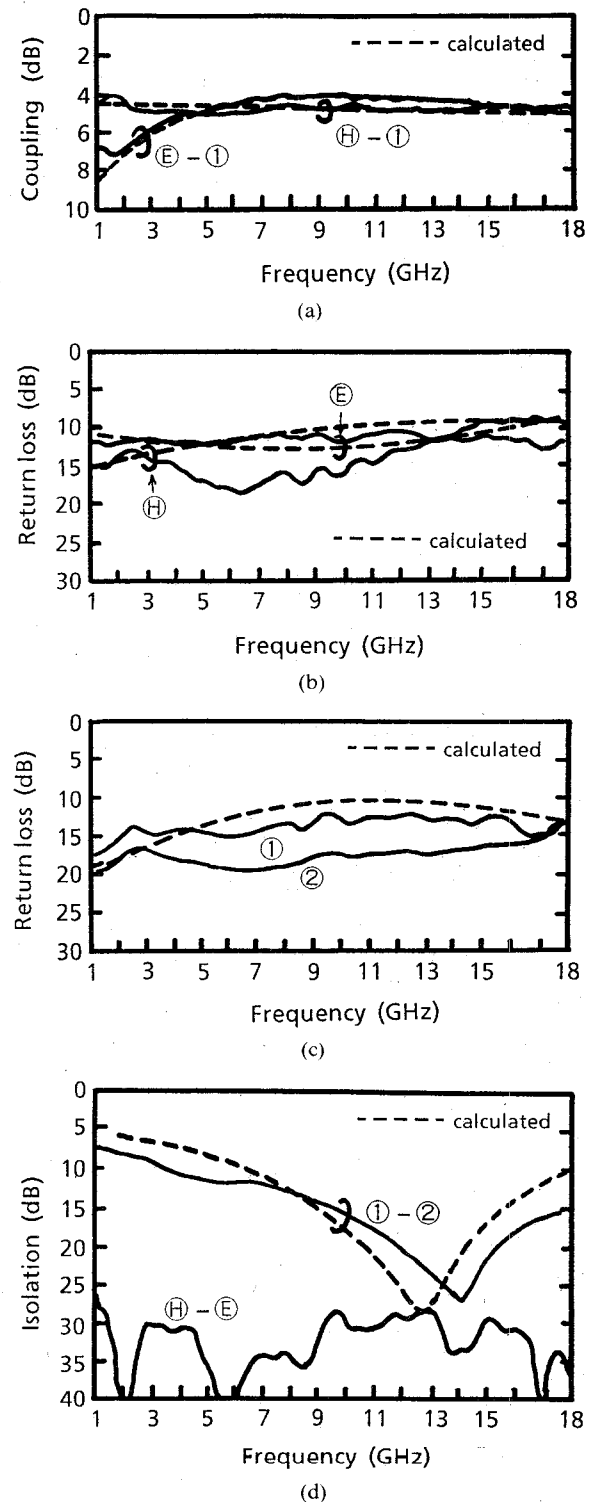


Fig. 11. Measured and calculated performance of the magic T. (a) Coupling between ports ④-①, ④-②, and ④-①, ②. (b) Return loss at ports ④ and ④. (c) Return loss at ports ① and ②. (d) Isolation between ports ①-② and ④-④.

$\text{mm}^2$ ). A chip area about 1/10 the size of a conventional magic T is achieved.

The measured performance of the fabricated thin-film MMIC magic T is shown in Fig. 11. The following performance is obtained in the frequency range from 4 to 18 GHz: coupling losses between ports ④-①/② and

between  $(H)-\textcircled{1}/\textcircled{2}$  are better than 5 dB; isolation between ports  $(E)-\textcircled{H}$  and ports  $\textcircled{1}-\textcircled{2}$  is better than 30 dB and 12 dB, respectively. The return loss at each port is better than 10 dB in the same frequency range. The coupling losses include the intrinsic loss (3 dB). The return loss characteristic at port  $(E)$  is improved by the loss characteristics of the  $50\ \Omega$  TFMS line on the  $3\text{-}\mu\text{m}$ -thick SiON film. Close agreement is obtained between the measured and calculated results. Thus, there is no effect on the TFMS bends in the meanderlike configuration. The insertion loss of about 2 dB will be reduced by increasing the film thickness to  $6\ \mu\text{m}$ .

## VI. CONCLUSION

A very small wide-band MMIC magic T ( $180^\circ$  hybrid circuit) using thin-film microstrip (TFMS) lines has been developed. The experimental results of the TFMS are described, and a model of the TFMS line is proposed. Loss characteristics and size estimation of the TFMS line are presented. TFMS is shown to effectively reduce the chip size, and by using a  $6\text{-}\mu\text{m}$ -thick SiON film the TFMS loss performance is almost the same as that of a conventional microstrip line on a  $100\text{-}\mu\text{m}$ -thick GaAs substrate. An MMIC magic T with an impedance of  $50\ \Omega$  at each port has been designed and fabricated. Very wide band performance and small size have been obtained.

The magic T described in this paper can be effectively used for small-sized, high-performance MMIC's and is expected to have wide applications in the microwave and millimeter-wave band. This technology can be extended to multilayer MMIC's, which consist of several thin dielectric films.

## ACKNOWLEDGMENT

The authors would like to thank Dr. K. Habara, Executive Vice President of Advanced Telecommunications Research Institute International (ATRI), and Dr. Y. Furuhama, President of ATR Optical and Radio Communications Research Laboratories, for their stimulating encouragement.

## REFERENCES

- [1] M. Aikawa and H. Ogawa, "A new MIC magic-T using coupled slot lines," *IEEE Trans. Microwave Theory Tech.*, vol. MTT-28, pp. 523-528, June 1980.
- [2] F. C. de Ronde, "A new class of microstrip directional coupler," in *G-MTT Int. Microwave Symp. Dig.*, May 1970, pp. 184-186.
- [3] T. Hirota *et al.*, "Uniplanar MMIC hybrid—A proposed new MMIC structure," *IEEE Trans. Microwave Theory Tech.*, vol. MTT-35, pp. 576-581, June 1987.
- [4] T. Tokumitsu *et al.*, "Active isolator, combiner, divider, and magic-T as miniaturized function blocks," in *Proc. IEEE GaAsIC Symp.*, 1988, pp. 273-276.
- [5] T. Tokumitsu *et al.*, "Very small, ultra wideband MMIC magic-T and applications to combiners and dividers," in *Proc. IEEE GaAsIC Symp.*, 1989, paper JJ-3.
- [6] K. C. Gupta *et al.*, *Microstrip Lines and Slotlines*. Norwood, MA: Artech House, 1978.
- [7] R. A. Pucel *et al.*, "Losses in microstrip," *IEEE Trans. Microwave Theory Tech.*, vol. MTT-16, pp. 342-350, June 1968.
- [8] E. J. Denlinger, "Losses of microstrip lines," *IEEE Trans. Microwave Theory Tech.*, vol. MTT-16, pp. 513-522, June 1968.



**Takahiro Hiraoka** (M'87) was born in Oita, Japan, in 1960. He received the B.E. and M.E. degrees in electrical engineering from Oita University, Oita, Japan, in 1983 and 1985, respectively.

In 1985, he joined NTT Electrical Communication Laboratories, Yokosuka, Japan. He was engaged in research on GaAs MMIC's and their application to space-borne equipment for satellite communications. In 1987, he joined ATR Optical and Radio Communications Research Laboratories, Osaka, Japan, where he is currently engaged in research on highly integrated MMIC's for future digital mobile communications.

Mr. Hiraoka is a member of the Institute of Electronics, Information and Communication Engineers of Japan.



**Tsuneo Tokumitsu** (M'88) was born in Hiroshima, Japan, in 1952. He received the B.S. and M.S. degrees in electrical engineering from Hiroshima University, Hiroshima, in 1974 and 1976, respectively.

He joined the Yokosuka Electrical Communication Laboratories, Nippon Telegraph and Telephone Public Corporation, Yokosuka, in 1976, where he did research on microwave and millimeter-wave integrated circuits, MIC's, and MMIC's and worked on the development of onboard satellite equipment. In September 1986 he joined ATR Optical and Radio Communications Research Laboratories, Osaka, where he is currently engaged in research on highly integrated MMIC's for future digital mobile considerations.

Mr. Tokumitsu is a member of the Institute of Electronics, Information and Communication Engineers of Japan.



**Masayoshi Aikawa** (M'78) was born in Saga, Japan, on October 16, 1946. He received the B.S., M.S., and Dr.Eng. degrees in electronics engineering from Kyushu University, Fukuoka, Japan, in 1969, 1971, and 1985, respectively.

In 1971, he joined the Musashino Electrical Communication Laboratories, Nippon Telegraph and Telephone Public Corporation, Tokyo, Japan, where he did research and development work on microwave and millimeter-wave integrated circuits, MIC's, MMIC's and equipment for 20 GHz digital radio trunk transmission systems and 26 GHz subscriber radio systems. In 1986, he joined ATR Optical and Radio Communications Research Laboratories, Osaka, Japan, where he was engaged in research on basic techniques for future digital mobile communications. He is now with the NTT Radio Communication Systems Laboratories, Yokosuka, where he has been engaged in research and development on monolithic microwave and millimeter-wave integrated circuits and their applications.

Dr. Aikawa is a member of the Institute of Electronics, Information and Communication Engineers of Japan.